AIAA Propulsion and Energy Forum
19-22 August 2019, Indianapolis, IN
AIAA Propulsion and Energy 2019 Forum

10.2514/6.2019-4503

Fault Detection and Identification for Multirotor Aircraft by Data-Driven and Statistical Learning Methods

Airin Dutta*, Michael E. McKay †, Fotis Kopsaftopoulos ‡, and Farhan Gandhi §
Center for Mobility with Vertical Lift (MOVE), Rensselaer Polytechnic Institute, Troy, NY, 12180

This work compares different data-driven methods for fault detection and identification of rotor failures in multicopters. The fault detection and identification methods employed in this study are based on response-only signals of the aircraft state, as the external excitation due to ambient turbulence is non-observable. Knowledge based methods using the knowledge of aircraft dynamics in the event of rotor failure is studied. A concise overview of the development of statistical time series models using the aircraft attitudes and statistical hypothesis testing to detect and classify rotor failures is presented. These methods are compared with neural networks trained on different parts of the response signals to achieve online fault detection identification of rotor failures in a hexacopter with respect to speed and accuracy of fault classification. It is shown that using a combination of statistical time series model for healthy aircraft and neural networks employed for online monitoring results in fault detection and identification in less than 0.3 s with an accuracy of 99.3%.

I. Nomenclature

α	=	Type I risk level
β	=	Type II risk level
γ	=	Autocorrelation
τ	=	Lag
σ^2	=	Residual variance
$\boldsymbol{\Sigma}$	=	Residual covariance matrix
ARMA	=	AutoRegressive Moving Average
$E\{\cdot\}$	=	Expected value
PE	=	Prediction Error
ARX	=	AutoRegressive with eXogenous excitation
PSD	=	Power Spectral Density
BIC	=	Bayesian Information Criterion
RSS	=	Residual Sum of Squares
FRF	=	Frequency Response Function
ACF	=	Auto-Covariance Function
CCF	=	Cross-Correlation Function
iid	=	Identically Independently Distributed
SPP	=	Samples Per Parameter
LS	=	Least Squares
SPRT	=	Sequential Probability Ratio Test
SSS	=	Signal Sum of Squares
AR	=	Scalar AutoRegressive model
VAR	=	Vector AutoRegressive model
FDI	=	Fault Detection and Identification

*Graduate Research Assistant, Mechanical, Aerospace, and Nuclear Engineering, AIAA Student Member
†Graduate Research Assistant, Mechanical, Aerospace, and Nuclear Engineering, AIAA Student Member
‡Assistant Professor, Mechanical, Aerospace, and Nuclear Engineering, AIAA Senior Member
§Redfern Chair Professor in Aerospace Engineering, MOVE Director, Mechanical, Aerospace, and Nuclear Engineering, AIAA Associate Fellow

II. Introduction

Multicopters, being capable of hovering and vertical take-off and landing, have attracted the interest of the community with respect to both commercial and defense applications over the last decade. Given the increasing interest and widespread use of these vehicles in a number of important arenas, early fault detection and identification of such systems are critical in order to ensure and improve their overall safety and reliability.

Rotorcraft are complex systems that exhibit strong dynamic coupling between rotors, fuselage, and control inputs, as well as time-varying and cyclo-stationary behavior. As a result, they face certain system modeling and fault detection and identification challenges that are not present in fixed-wing aircraft. These issues, as well as potential solutions, have been explored in the recent literature.

An algorithm for online detection of motor failure using only inertial measurements and control allocation by an exact redistributed pseudo-inverse method for octacopters has been demonstrated by Frangenberg et al. [1]. Heredia and Ollero [2] have addressed sensor fault identification in small autonomous helicopters using Observer/Kalman Filter identification. Fault tolerant control for multi-rotors [3, 4], as well as various fault diagnosis methods such as analytical models, signal processing, and knowledge-based approaches for helicopters have also been proposed [5].

Statistical time series methods have been used to detect various fault types in aircraft control systems due to their simplicity, efficient handling of uncertainties, no requirement of physics based models, and applicability to different operating conditions [6–9]. Dimogianopoulos et al. [10] have demonstrated the effectiveness of two statistical schemes based on Pooled Non-Linear AutoRegressive Moving Average with eXogenous excitation (P-NARMAX) to detect and isolate faults for aircraft systems under different flight conditions, turbulence levels, and fault types and magnitudes. The first method models the pilot input and aircraft pitch rate relationship, while the second approach models the relationship between horizontal and vertical acceleration, angle of attack and pitch rate signals in fixed-wing aircraft. Ganguli et al. [11] have trained neural networks with noise-contaminated simulated vibration and response data to detect and quantify single and multiple faults on damaged helicopter rotor blades. Morel et al. [12] employed neural networks for classification of vibration signatures generated by a parametric model of a helicopter to detect and trace defects on helicopter rotors.

Online fault detection in multicopters using statistical time series methods to achieve early detection of rotor failures in the presence of external disturbances, such as different levels of turbulence and uncertainty, has been achieved [13]. The objective of the present study is to identify faults by various data-driven methods including time-series modeling and neural networks, and compare them with respect to their accuracy in classifying faults. This information will be extremely useful for control allocation redistribution and reconfiguration of the vehicle to accomplish safe flight.

III. Hexacopter Model and Data Generation

A. Physics-Based Modeling of Multicopter System

A flight simulation model has been developed for a regular hexacopter (Fig. 1) using summation of forces and moments to calculate aircraft accelerations. This model is used as the main source of simulated data under varying operating and environmental conditions, as well as different fault types. Rotor loads are calculated using Blade Element Theory coupled with a 3×4 Peters-He finite state dynamic wake model [14]. This model allows for the simulation of abrupt rotor failure by ignoring the failed rotor inflow states and setting the output rotor forces and moments to zero.

A feedback controller is implemented on the nonlinear model to stabilize the aircraft altitude and attitudes, as well as track desired trajectories written in terms of the aircraft velocities. This controller is designed at multiple trim points, with gain scheduling between these points to improve performance throughout the flight envelope.

The state vector consists of the 12 rigid body states and is defined in Eq. (1).

$$\mathbf{x} = \begin{Bmatrix} X & Y & Z & \phi & \theta & \psi & u & v & w & p & q & r \end{Bmatrix}^T \tag{1}$$

The input vector is comprised of the first four independent multirotor controls for collective, roll, pitch and yaw and is defined in Eq. (2):

$$\mathbf{u} = \begin{Bmatrix} \Omega_0 & \Omega_R & \Omega_P & \Omega_Y \end{Bmatrix}^T \tag{2}$$

The control architecture is illustrated in Fig. 2 and detailed in Ref. 3. This control design has been demonstrated to perform well even in the event of rotor failure, with no adaptation in the control laws themselves.

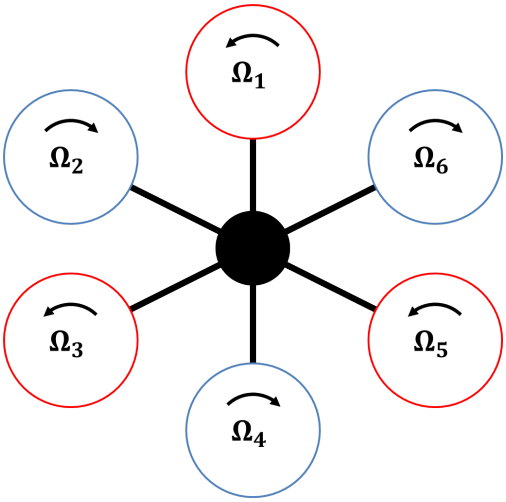

Fig. 1 Schematic representation of a regular hexacopter

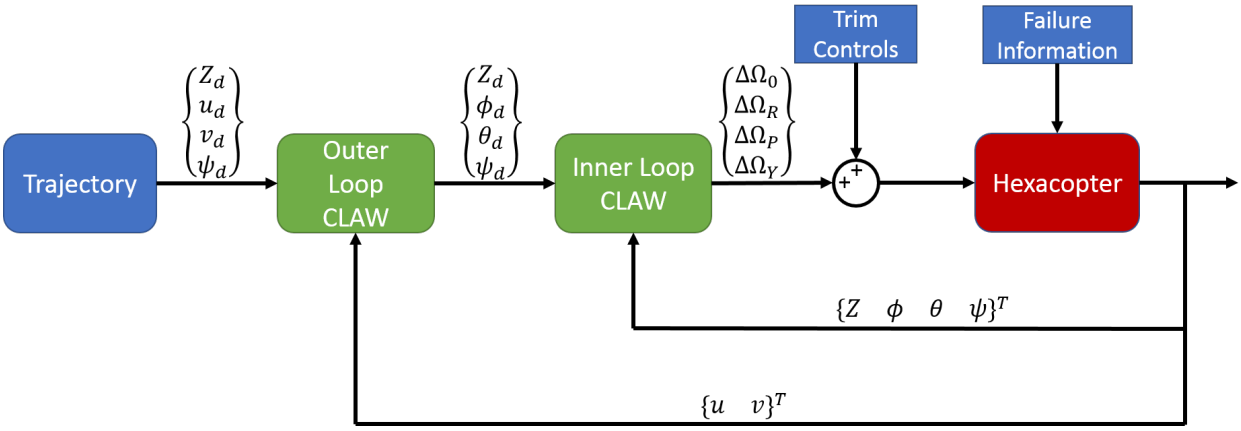

Fig. 2 Controller block diagram

B. Data Generation

A continuous Dryden wind turbulence model [15] has been implemented in the flight simulation model. The Dryden model is dependent on altitude, length scale, and turbulence intensity and outputs the linear and angular velocity components of continuous turbulence as spatially varying stochastic signals. The proper combination of these parameters determines the fit of the signals to observed turbulence.

Table 1 Simulation Data

Aircraft state	Number of datasets for turbulence levels		
	Light	Moderate	Severe
Healthy	100	100	100
Rotor failure (1)	100	100	100
Rotor failure (2)	100	100	100
Rotor failure (6)	100	100	100
Sampling frequency: f_s = 100 Hz			
Signal length in samples: N = 8000 (80 s)			

In this system, altitude is taken as 5m and the length scale as the hub-to-hub distance of the hexacopter, which is 0.6096 m (2 ft). The data sets for aircraft states are generated through a series of simulations for different turbulence levels (light, moderate and severe) both for healthy aircraft and different fault types, such as failure of front or side rotors. For a summary of the generated data sets see Table 1. The time series (signals) of the hexacopter attitudes (aircraft states) for the healthy state, as well as for different fault types, provide useful insight into the dynamics of the system which can be utilized in knowledge-based method fault detection identification [13]. A typical signal from flight simulation involves substantial transient behavior at the time of rotor failure, followed by a return to steady state as the controller compensates for the loss of a rotor. The rotor failures addressed in this work are: front rotor (rotor 1), right-side rotor (rotor 2), and left-side rotor (rotor 6) failure.

IV. Knowledge-based Fault Detection and Identification

From the knowledge of the dynamics of the hexacopter model, it can be inferred that failure of rotor 1, 2, or 6 (consequent loss of thrust) will result in sharp transients in roll, pitch and yaw attitudes of the aircraft at the time of failure.

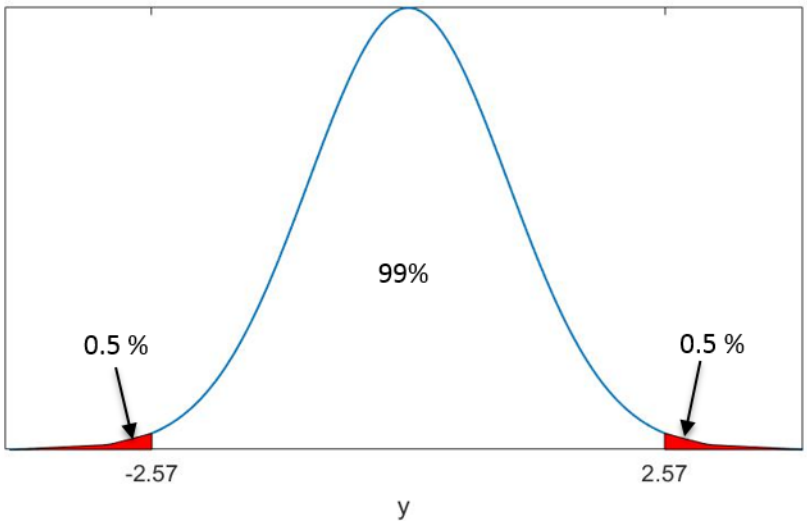

Fig. 3 Probability distribution for normally distributed data with 99% confidence intervals

The aircraft attitudes for healthy flight under different levels of turbulence follow a normal distribution as shown in Fig. 3. The 99% confidence interval for each signal,$y[t]$ (roll, pitch and yaw attitudes) is calculated by Eq. (3):

$$\begin{aligned} \text{Upper bound} &= E(y) + 2.576 \times \sqrt{E(y^2)} \\ \text{Lower bound} &= E(y) - 2.576 \times \sqrt{E(y^2)} \end{aligned} \tag{3}$$

where, $E(y)$ and $E(y^2)$ are the expected value (mean) and variance of the signals recorded over 60 s of healthy flight under severe turbulence.

The behavior of the aircraft transient response to rotor failure can help to identify the failure type using specific knowledge of the aircraft dynamics. Failure of rotors 1,2, or 6 cause the aircraft to pitch nose-down due to loss of thrust, marking an event of rotor failure. The heading of the aircraft deviating in different directions for front rotor (rotor 1) failure compared to side rotor failure (rotor 2 and 6), helps classify between front or side rotor failure. This is due to the different rotor spin directions, and consequently the direction of the hub torque generated by each rotor. Finally, front rotor (rotor 1) failure, does not significantly affect the aircraft roll equilibrium. However, in the case of side rotor (rotor 2 or 6) failure, roll attitudes deviate in opposite directions as the aircraft rolls in the direction of the failed rotor due to its loss of thrust. The knowledge-based fault detection and identification thus follows decision making process depicted in the following flowchart (Fig. 4).

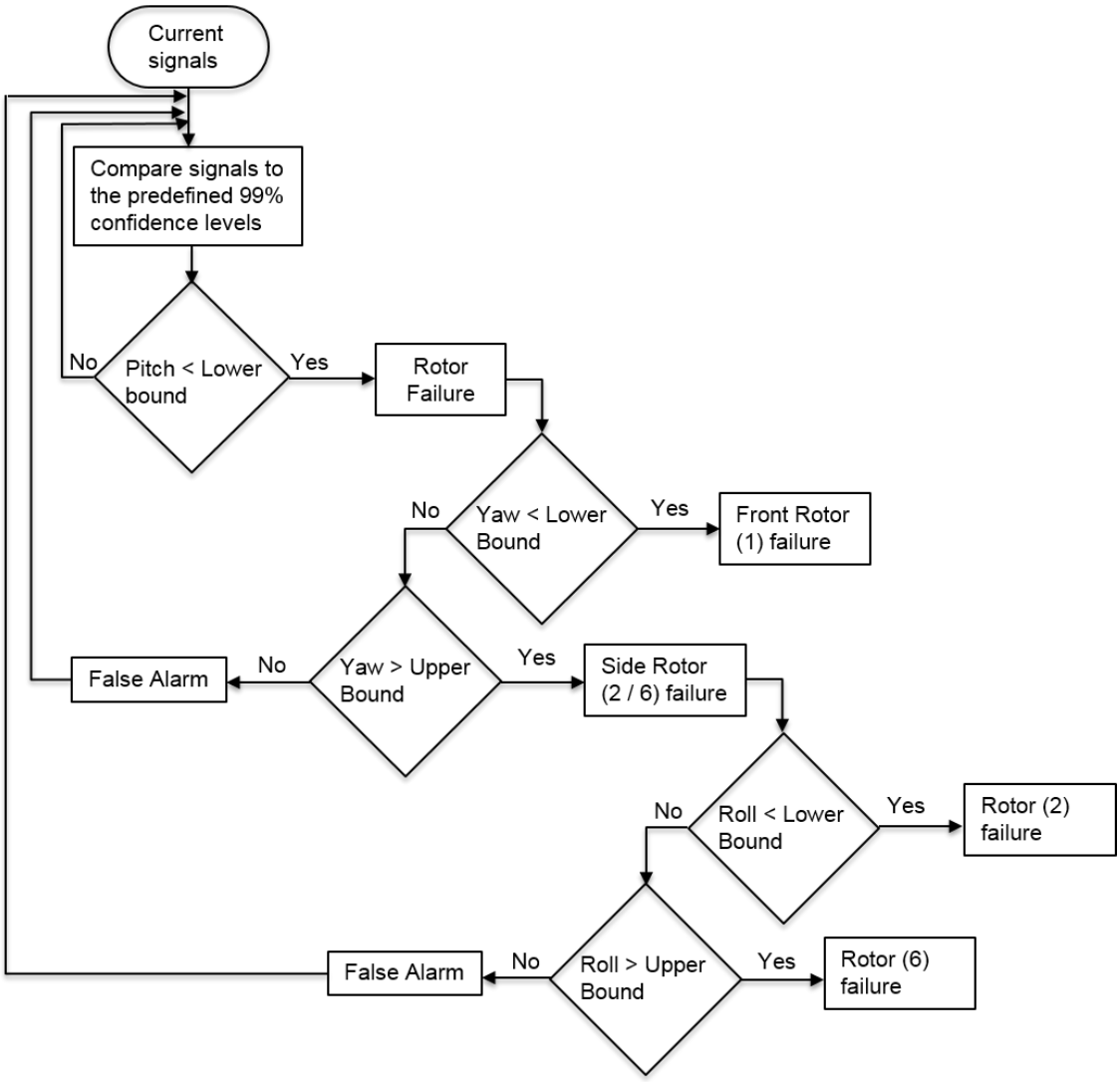

Fig. 4 Flowchart for knowledge-based fault detection and identification

V. Statistical Time-Series Method for Fault Detection and Identification

The aircraft signals for roll, pitch and yaw attitudes generated via a series of simulations of forward flight of the hexacopter under turbulence (light, moderate and severe levels) for healthy and different faulty states are used for model identification and fault detection and identification.

In the present scenario, the signals obtained are response only signals with the excitation $x[t]$ assumed to be a white (uncorrelated) signal induced by atmospheric turbulence. That is $\gamma_{xx}[\tau] = 0$ for $\tau \neq 0$, where γ_{xx} denotes the AutoCorrelation Function (ACF) and τ the ACF time lag, given as:

$$\gamma_{xx}[\tau] = E\{x[t] \cdot x[t+\tau]\} \tag{4}$$

A. Parametric Identification via Time Series Models

It has been shown that Vector Auto-Regressive models perform better than Scalar Auto-Regressive models with respect to number of false alarms and tolerance to different levels of turbulence [13]. Hence, VAR models for healthy aircraft and the different rotor failures have been estimated and used in the present study.

1. Vector AR Model Identification

Vector AutoRegressive (VAR) models employ s-dimensional signals, i.e. the aircraft states in the present study, for multivariate (s-variate) time series modeling [16, 17]. Though they bear striking resemblance to their univariate or scalar counterparts, they have a much richer structure and typically require multivariate statistical decision making procedures. The multi-variate response signal $\mathbf{y}[\mathbf{t}]^*$ obtained from a flight simulation is parametrized to form VAR(na) model is of the following form:

$$\begin{aligned} \mathbf{y}[t] + \sum_{i=1}^{na} \mathbf{A}_i \cdot \mathbf{y}[t-i] = \mathbf{e}[t], \quad \text{with} \\ \mathbf{e}[t] \sim \text{iid } N(\mathbf{0}, \boldsymbol{\Sigma}), \quad \boldsymbol{\Sigma} = E\{\mathbf{e}[t] \cdot \mathbf{e}^T[t]\} \end{aligned} \tag{5}$$

where $\mathbf{A}_i$ $(s \times s)$ designates the i-th AR matrix, $\mathbf{e}[t]$ $(s \times 1)$ the model residual sequence characterized by the non-singular and generally non-diagonal covariance matrix $\boldsymbol{\Sigma}$, na the AR order, and $E\{\cdot\}$ statistical expectation.

The identification of parametric time series models is comprised of two main tasks: parameter estimation and model order selection. Given the attitude signal measurements $y[t]$ $(t = 1, 2, \ldots, N)$, the estimation of the VAR parameter vector $\boldsymbol{\theta}$ comprising all AR matrix elements ($\boldsymbol{\theta} = \text{vec}([\mathbf{A}_1\mathbf{A}_2 \ldots \mathbf{A}_{na}])$ and the residual covariance matrix $\boldsymbol{\Sigma}$ is accomplished via linear regression schemes based on minimization of the Ordinary Least Squares (OLS) or the Weighted Least Squares (WLS) criterion [18, 19]. The modeling procedure involves the successive fitting of VAR(na) models for increasing AR order na, and examining of the Bayesian Information Criterion (BIC) [7, 18, 19] and Residual sum of Squares over Signal Sum of Squares Criterion (RSS/SSS). The former is a statistical criterion that penalizes model complexity (order, and hence the number of free parameters) as a counteraction to a decreasing model fit criterion. The latter determines the predictive capability of the model.

B. Residual Based Fault Detection and Identification

For fault detection and identification, model residual based methods use functions of the residual sequences (known as characteristic quantity) which are obtained by driving the current signal(s) (Z_u) through the models estimated in the baseline phase for the healthy aircraft (M_o) and different fault types (M_1, M_2, M_6). The key idea is that the residual sequence obtained by a model that truly reflects the current state of aircraft possesses certain distinct properties which are distinguishable from that obtained from the other models.

Let M_V designate the model representing the structure in its V state ($V = 0, 1, 2, 6$), where '0' denotes healthy state and $1, 2, 6$ signify the rotor which has failed in the faulty state. The residual series obtained by driving the current signal(s) (Z_u) through each one of the aforementioned models are designated as $e_{0u}[t], e_{1u}[t], e_{2u}[t], e_{6u}[t]$ and are characterized by variances $\sigma^2_{0u}, \sigma^2_{1u}, \sigma^2_{2u}, \sigma^2_{6u}$ respectively. The first subscript designates the model employed, while the second the aircraft state corresponding to the currently used response signal(s). The characteristic quantities obtained from the corresponding residual series are designated as $Q_{0u}, Q_{1u}, Q_{2u}, Q_{6u}$. The characteristic quantities obtained using the baseline data records are designated as $Q_{VV}(V = 0, 1, 2, 6)$.

1. Residual Uncorrelatedness Method

This method is based on the fact that the residual series $e_{ou}[t]$, obtained by driving the current signals (Z_u) through the model (M_0), is uncorrelated (white) if and only if the aircraft is currently in its healthy condition [6]. Fault detection is performed by the following hypothesis testing:

$$\begin{aligned} \text{H}_0 \quad &: \rho[\tau] = 0 \quad \text{(null hypothesis – healthy aircraft)} \\ \text{H}_1 \quad &: \rho[\tau] \neq 0 \quad \text{(alternate hypothesis – rotor failure)} \end{aligned} \tag{6}$$

where $\rho[\tau]$ is the normalized autocorrelation function ($\rho_{xx}[\tau] = \gamma_{xx}[\tau]/\gamma_{xx}[0]$) of the residual sequence $e_{ou}[t]$.

Therefore, the characteristic quantity for fault detection by this method is $\left[\rho[1]\ \rho[2]\ \rho[3] \ldots\ \rho[\tau]\right]^T$. For this method, r is the design variable for the statistical test, which denotes the maximum lag in time (τ) for which the normalized ACFs are being accounted for. Under the null hypothesis (H_0), the residuals $e_{ou}[t]$ are iid Gaussian with

*Bold–face upper/lower case symbols designate matrix/column–vector quantities, respectively. Matrix transposition is indicated by the superscript ^{T}.

zero mean and the test statistic χ^2_ρ follows a χ^2 distribution with r degrees of freedom, given as:

$$\text{Under } H_0 : \chi^2_\rho = N(N+2) \cdot \sum_{\tau=1}^{r} (N-\tau)^{-1} \cdot \widehat{\rho}[\tau]^2 \sim \chi^2(r) \tag{7}$$

where $\widehat{\rho}[\tau]$ denotes the estimator of $\rho[\tau]$.

Statistical decision making is achieved by the following test for α (false alarm) risk level:

$$\begin{array}{ll} \chi^2_\rho \leq \chi^2_{1-\alpha}(r) & \Rightarrow H_0 \text{ is accepted (healthy aircraft)} \\ \text{Else} & \Rightarrow H_1 \text{ is accepted (rotor failure)} \end{array} \tag{8}$$

where $\chi^2_{1-\alpha}(r)$ denotes the χ^2 distribution's $1-\alpha$ critical point.

Fault identification is achieved by similarly examining which one of the $e_{Vu}[t](V = 1, 2, 6)$ residual series is statistically uncorrelated. A schematic representation of residual based fault detection identification has been illustrated in Fig. 5.

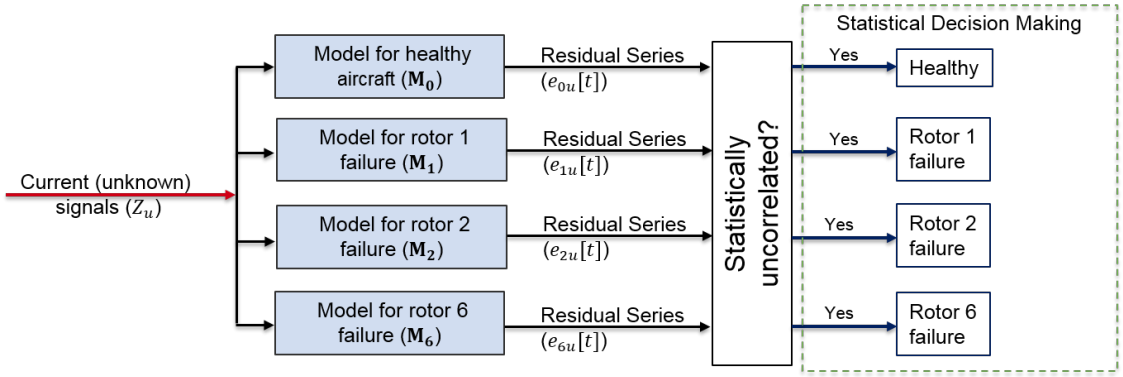

Fig. 5 General workframe of residual based statistical time series based fault detection and identification

VI. Neural networks based Fault Detection and Identification

The aircraft attitude signals have two distinct behavior in case of failure: transient and fault compensated state. Neural Networks with single hidden layer are effective in classifying the faults with significantly less computation time, ideal for online monitoring when trained on either transient or steady state signals separately. A single neural network trained on both transient and steady state signals has shown considerable misclassification and longer time to detect and classify faults. Hence, to achieve faster and effective fault detection identification with minimum false alarms and misclassification errors, two neural networks have been trained:

1) **Neural network 1**: This network has 4 output classes, namely healthy and rotor 1, 2, or 6 failures. It is trained over transient roll, pitch and yaw attitude signals of very short length generated at the instant of time of rotor failure and a healthy signal of same length. Since the transient signals have distinctive properties relating to each rotor failure as described in Section IV, they are suitable for fast fault detection and classification. Here, the speed of detection depends on length of signals used to train the network. Hence, it has been selected by rigorous testing to minimize false alarms, missed faults and fault misclassification.
2) **Neural network 2**: This network classifies rotor faults 1, 2, or 6 from post-failure compensated steady state signals. It has been observed that using attitude signals to train this network results in poor classification. To overcome this difficulty, the statistical time series model for healthy aircraft (M_0) (Section V.B) has been used to filter the current signals and generate roll, pitch and yaw residual sequences. The cross-correlation function (Eq. 9) between the different residuals exhibits trends as shown in Figs. 15 to 17 that can be used for classification of faults. The cross-correlation function between two signals $z(t)$ and $x(t)$, denoted by $\gamma_{xx}[\tau]$ is given by Eq. 9.

$$\gamma_{zx}[\tau] = E\{z[t] \cdot x[t+\tau]\} \tag{9}$$

where, τ is the time lag in number of samples.

This method improves the accuracy of neural network considerably. Even with shorter signal lengths (compared to training by attitude signals), the accuracy does not deteriorate, making it better suited for online monitoring. This is discussed in Section VII.C.

Online fault detection and identification using neural networks has been achieved through the flowchart depicted in Fig. 6. Current signals are passed through Neural network 1 to detect faults by continuous monitoring. In an event of rotor failure, the transient signals are used to identify the fault. Next, the variance of the signals is used to check whether they have reached steady state or not. It can be observed that transient signals exhibit large variance, whereas in steady state, the variance in the signals of interest is much lower. Thereafter, the residuals generated from filtering the steady state signals through healthy model (M_0) are used for online identification of faults by Neural network 2.

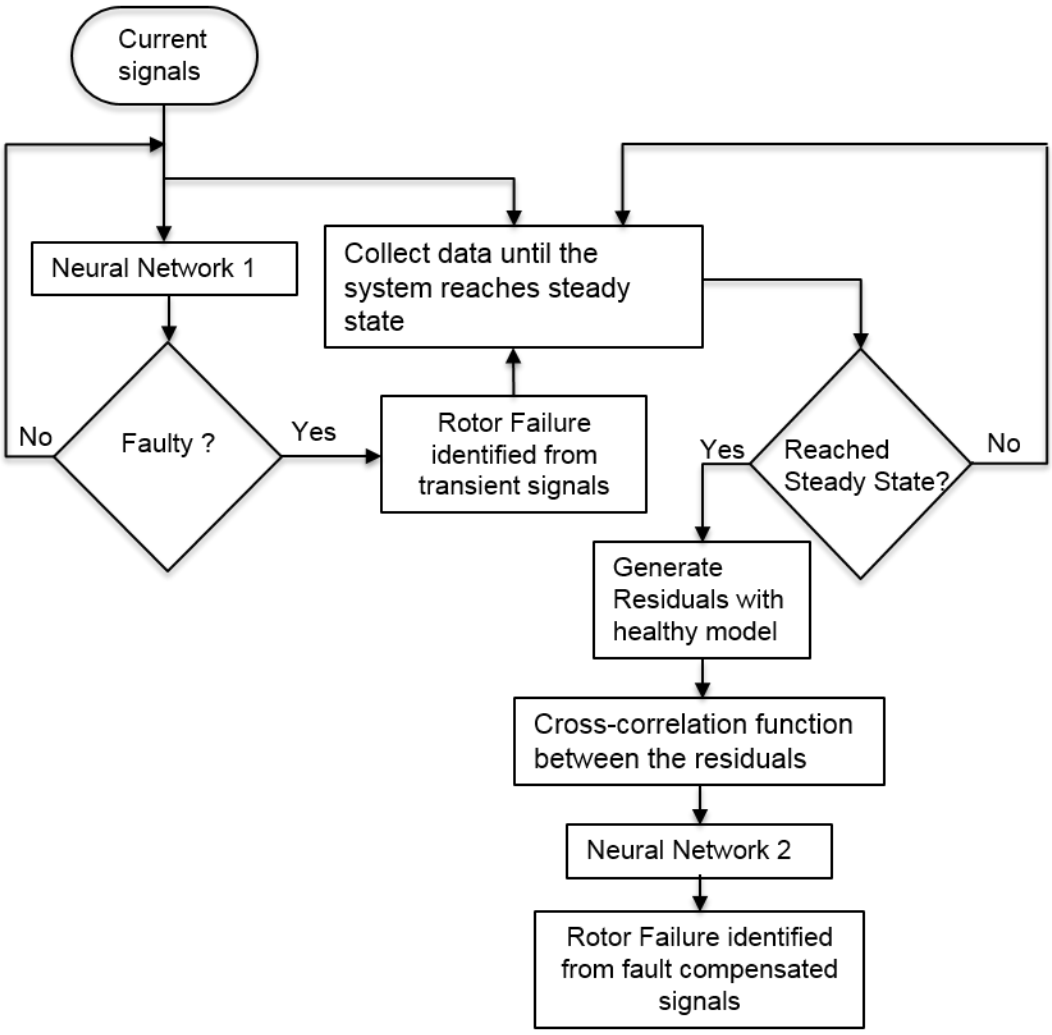

Fig. 6 Flowchart of neural network based fault detection and identification

VII. Results and Discussion

A. Knowledge based Fault Detection and Identification

The signals are sampled at a frequency of 100 Hz and online monitoring is performed following the algorithm depicted in Fig. 4. At the instant of rotor failure the signals deviate from their 99% confidence interval as shown in enlarged view in Fig. 7. From the directions in which the signals deviate, the rotor failure is detected and identified within a maximum and average time of 0.7s and 0.1s respectively. The computation time is less than 0.0009 s, which is less than the sampling time of 0.01 s. Once a fault is identified, the process terminates. Hence, there will be only one decision per simulated flight data set. The summary of results for fault detection and fault classification using the knowledge based approach are given in Table 2 and 3.

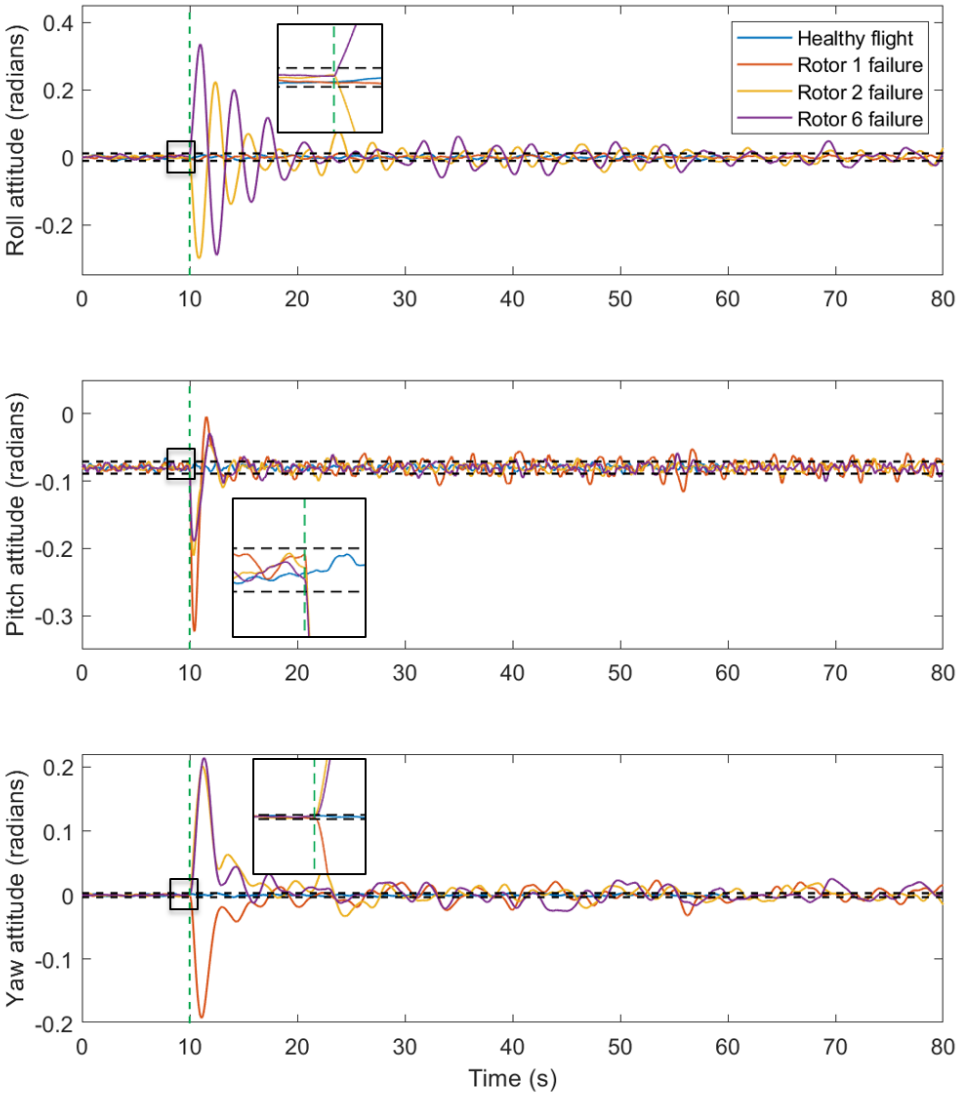

Fig. 7 Roll, pitch and yaw attitude signals for an airspeed of 5 m/s under severe turbulence. The green dashed vertical line indicates the instant of rotor failure and the black dashed horizontal lines indicates the 99% confidence intervals.

Table 2 Fault Detection results for Knowledge based FDI

Healthy	Failure cases		
	Rotor 1	Rotor 2	Rotor 6
False Alarms	Missed Faults		
2/3/0	0/0/0	0/0/0	0/0/0

False Alarms for severe/moderate/light levels of turbulence out of 100 cases each
Missed Faults for severe/moderate/light levels of turbulence out of 100 cases each

Table 3 Confusion Matrix for Fault Classification by Knowledge based FDI

		Signals for failure of		
		Rotor 1	Rotor 2	Rotor 6
Outputs	Rotor 1	100/100/100	0/0/0	0/0/0
	Rotor 2	0/0/0	100/100/100	0/0/0
	Rotor 3	0/0/0	0/0/0	100/100/100

Fault Classification for severe/moderate/light levels of turbulence out of 100 cases each

B. Statistical Time-Series Method for Fault Detection and Identification

1. Vector AR Model Identification

Vector (multivariate) parametric identification of the healthy aircraft has been based on 20 s ($N = 2000$ samples at sampling frequency 100 Hz) data sets for the roll, pitch, and yaw signals, without any external excitation (ambient excitation due to turbulence assumed to be white) generated from forward flight simulation at 5 m/s under severe turbulence.

Model order selection is based on a combination of Bayesian Information Criteria (BIC) and Residual sum of squares normalized by Signal sum of squares (RSS/SSS) criteria as shown in Fig. 8. A model order of $na = 4$ yields the minimum BIC for healthy aircraft and this model is represented as M_0. Monitoring the stabilization of RSS/SSS criteria gives the point where increasing model order does not result further in reduction of prediction errors. This order exhibits a very low RSS/SSS value of $2.5 \times 10^{-5}\%$ demonstrating accurate identification and excellent dynamics representation of the healthy aircraft attitude signals at 5 m/s and under severe turbulence. The samples per parameter (SPP) for the model is 166.67 as the number of estimated parameters for VAR(4) is 36 (as the $\boldsymbol{A}_i$ parameter matrix is a 3×3 matrix with $i = 1, 2, 3, 4$ for model order of 4). The roll, pitch and yaw signals of the healthy aircraft flying at 5 m/s for different turbulence realization have been driven through the estimated healthy model estimated to generate residuals. The autocorrelation and cross-correlation functions of the three residual sequences generated are observed to be white with 95% confidence as shown in Fig. 9. For signals generated for different faulty states, the residuals are found to be correlated. This provides validation of the estimated model, M_0, that it is capable of representing the dynamics of a healthy aircraft under the considered flight conditions.

Similarly, vector (multivariate) parametric identification of different rotor failure models have been based on 20s ($N = 2000$ samples at sampling frequency 100 Hz) of steady state aircraft attitude signals after controller compensation obtained from forward flight simulation at 5 m/s under severe turbulence. Typically, the roll, pitch and yaw signals fully stabilize with different dynamics than the healthy state due to controller action after rotor failure. The details of the estimated models for the healthy and all faulty states of the aircraft using the three aircraft attitude signals are given in Table 4

2. Residual based fault detection and identification

The current (unknown) signals (roll, pitch and yaw in that order), when driven through the healthy model (M_0) estimated in the previous section, yield three sets of residual sequences.Therefore, the statistical hypothesis testing to determine whether the current residuals are uncorrelated or not is performed thrice for a particular time window (duration of signal measured in number of samples).

Table 4 Vector AR Models identification summary

Aircraft State	Model order	Parameters estimated	SPP
Healthy	VAR(4)	36	166.67
Rotor 1 failure	VAR(6)	54	111.11
Rotor 2 failure	VAR(8)	72	83.33
Rotor 6 failure	VAR(6)	54	111.11

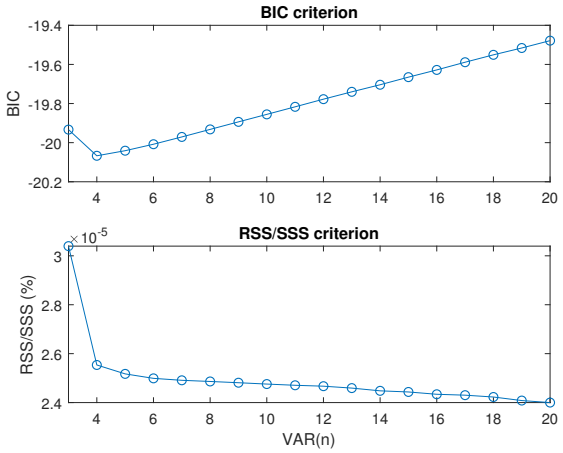

Fig. 8 Vector AR model order selection

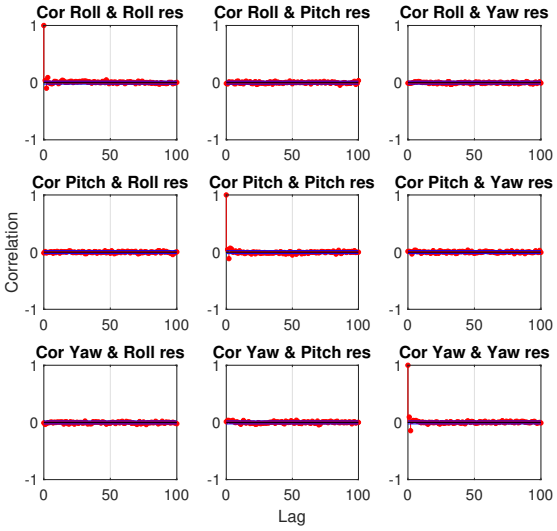

Fig. 9 Crosscorrelation of the roll, pitch and yaw residuals for healthy aircraft

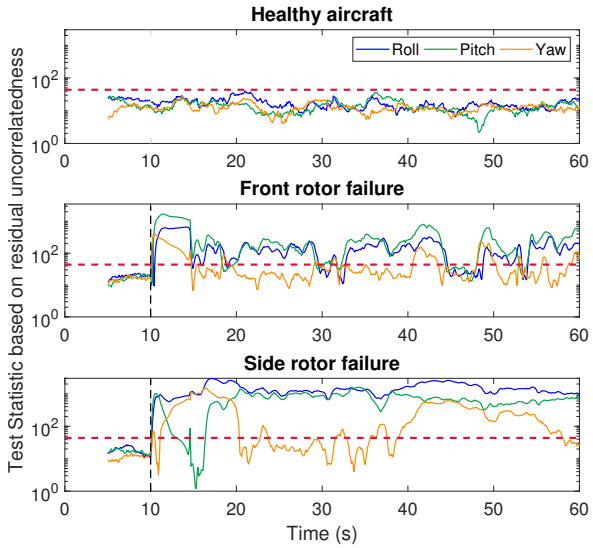

Fig. 10 Indicative residual uncorrelatedness based fault detection results. The dashed red horizontal line indicates the statistical threshold at the $\alpha = 10^{-3}$ risk level.

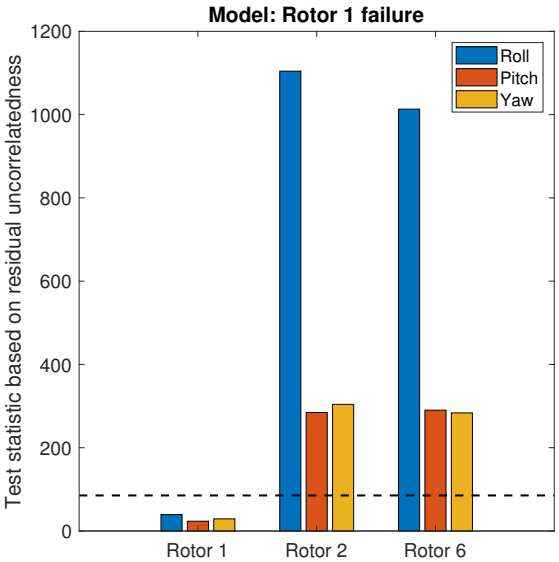

Fig. 11 Indicative residual uncorrelatedness based fault identification results. The dashed red horizontal line indicates the statistical threshold at the $\alpha = 10^{-3}$ risk level.

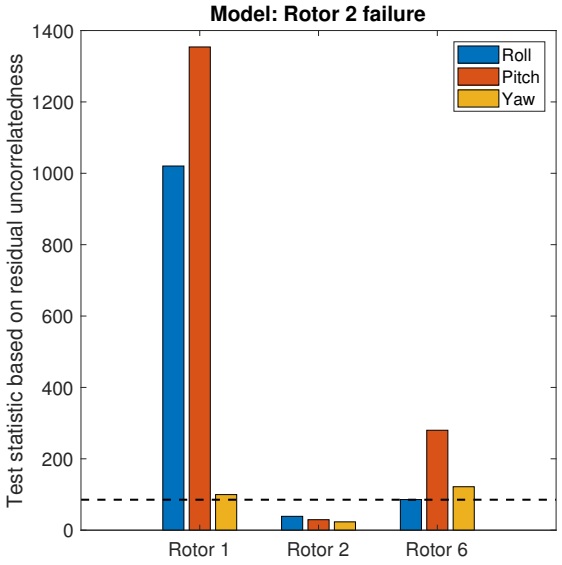

Fig. 12 Indicative residual uncorrelatedness based fault identification results. The dashed red horizontal line indicates the statistical threshold at the $\alpha = 10^{-3}$ risk level.

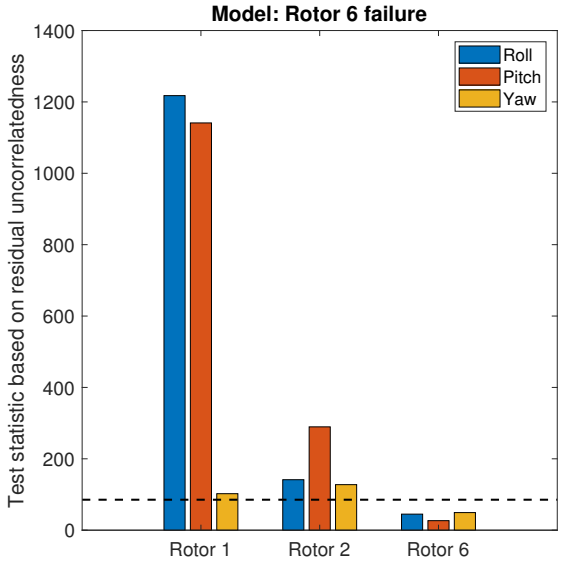

Fig. 13 Indicative residual uncorrelatedness based fault identification results. The dashed red horizontal line indicates the statistical threshold at the $\alpha = 10^{-3}$ risk level.

Online fault detection by residual uncorrelatedness is performed with 5 s ($N = 500$ samples) window length and update interval of 0.1 s for each residual sequence. Here, the autocorrelation function of each of the residuals with a maximum lag $\tau = 20$ are considered as the test statistics. The critical limit of the statistical hypothesis testing is given as the $(1 - \alpha)$ critical point of a χ^2 distribution with 20 degrees of freedom. Figure 10 shows three parallel hypothesis tests on roll, pitch and yaw residuals for different current states of the aircraft: healthy aircraft, front, and side rotor failure, respectively, at the risk level, α, of 10^{-3}.

In the healthy case, the test statistic for all the three signals is lower than the the critical limit, correctly indicating the system is healthy. For rotor failure at 10 s, fault detection is almost immediate. The test statistics for side rotor failure exceed the critical limit by a greater amount than in the case of front rotor failure due to significant change of all three signals (roll, pitch, and yaw) in the former compared to only two (roll and pitch) in the latter, as discussed. Even after fault compensation, all three test statistics continue to violate the critical limit, indicating a faulty system. Hence, the test is able to distinguish a healthy system from a fault compensated system from the changes in the three attitude signals of the aircraft. It should be noted that the test statistic for roll in the case of side rotor failure shows the maximum deviation, as the controller compensates it in an underdamped fashion [13].

Statistical time series models for different types of failures have been estimated to capture the dynamics of stationary, fault-compensated signals. When a fault is encountered, the variance of signals of window length 10 s, updated every 0.1 s, are evaluated. As depicted in Fig. 14, as the transients pass, the signal variance reduces considerably. This fact has been utilized to check whether steady state have been reached or not. The threshold values of variances for the roll, pitch and yaw signals, below which the signals are considered to have reached steady state, have been evaluated as the maximum variances for each signal encountered in the steady state (20s after instant of rotor failure) for 20 sets of simulation data, for each type of rotor failure and severe level of turbulence. The value of roll, pitch and yaw signals threshold variances are $1 \times 10^{-3} rad^2$, $1 \times 10^{-4} rad^2$ and $3 \times 10^{-4} rad^2$ respectively.

After the fault is compensated for by the controller, signals of length 20 s ($N = 2000$ samples), updated every 1 s have been filtered through faulty models M_1, M_2 and M_6 to generate residual sequences $e_{1u}[t], e_{2u}[t]$ and $e_{6u}[t]$ respectively, each containing roll, pitch and yaw residuals. The autocorrelation function of each component of the residual sequences with maximum lag $\tau = 50$ has been considered as the test statistics to classify faults. Since the computation time required to classify failure is about 0.3 s, the window update interval is kept at 1 s.

The results obtained from a single window of 20 s have been shown in Figs.11 to 13. Figure. 11 shows the residuals $e_{1u}[t]$ are uncorrelated (lies below $(1 - \alpha)$ critical limit of a χ^2 distribution with 50 degrees of freedom). This signifies that the model (M_1) represents the dynamics of current state correctly and hence the fault is classified as failure of

rotor 1. The models which do not represent the current aircraft state dynamics, have correlated residuals (violate the critical limit). Similarly, Figs. 12 and 13, show correct identification of the failure of rotor failure 2 and 6, respectively. It has been observed from Fig.11 that the extent of violation of critical limit is more in roll residuals than pitch and yaw residuals for side rotor failure. This is due to the fact that roll does not change significantly for front rotor failure as captured by model M_1, contrary to the case of side rotor failure. Also, in Figs. 12 and 13, the front rotor failure signals show a substantial pitch correlatedness compared to the other side rotor failure, which signifies that controller compensated pitch dynamics is significantly different in front rotor failure from side rotor failure as previously discussed in [13].

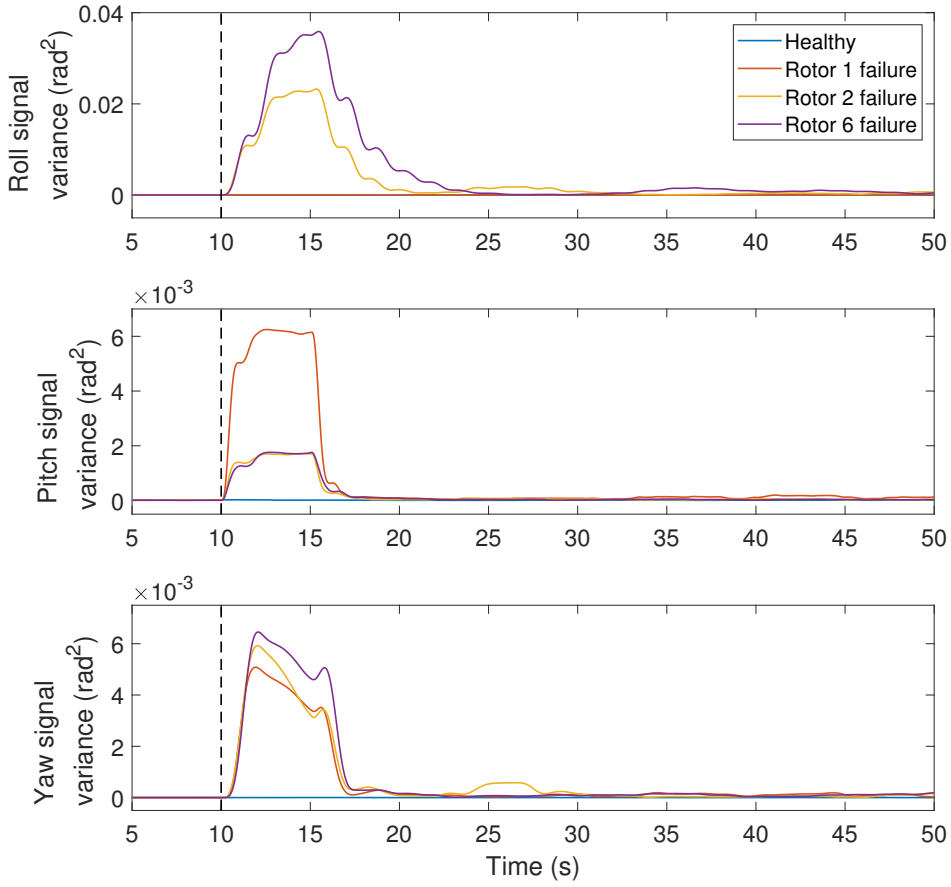

Fig. 14 Variances of roll, pitch and yaw signals

Table 5 Fault detection results for statistical time-series method

Healthy	Failure cases		
	Rotor 1	Rotor 2	Rotor 6
False Alarms %	Missed Faults		
0.16/0.018/0.24	0/0/0	0/0/0	0/0/0

False Alarms % for severe/moderate/light levels of turbulence
Missed Faults for severe/moderate/light levels of turbulence out of 100 cases each

The summary of results for fault detection using statistical time series models is given in Table 5. The signals to be

Table 6 Confusion matrix for fault classification by statistical time-series method

		Signals for failure of		
		Rotor 1	Rotor 2	Rotor 6
Models	Rotor 1	100/100/100	0/0/0	0/0/0
	Rotor 2	0/0/0	99.45/99.57/99.86	0.061/0/0
	Rotor 3	0/0/0	0/0/0	99.57/99.78/99.70

Fault Classification for severe/moderate/light levels of turbulence in percentage

correctly classified as a particular fault type, all the 3 test statistics for the roll, pitch and yaw residuals obtained from filtering through the model estimated for that particular fault type, should be below the critical limit. The summary of results for fault classification by statistical time series method is given in Table 6. The diagonal elements of this table represents the correct identification of the rotor failures and the off-diagonal elements shows the classification errors.

C. Neural networks based Fault Detection and Identification

1. Training neural networks

Neural network 1 is trained with 60 sets of 0.2 s transient roll, pitch and yaw signals from the instant of rotor failure for each type of failure and levels of turbulence. The data with a healthy target (or output classification) is trained with 60 sets of same length of roll, pitch and yaw signals from a random instant within the simulation data for healthy flight. Signals with lesser length will enable faster detection but with reduced accuracy with respect to fault classification.

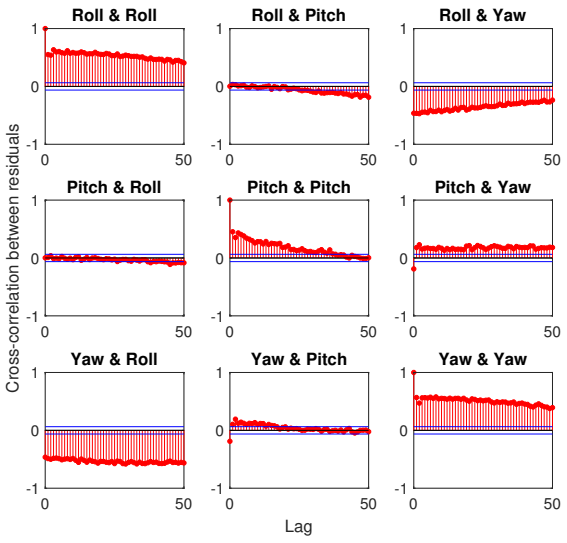

Fig. 15 Crosscorrelation of the roll, pitch and yaw residuals generated by healthy aircraft model for rotor 1 failure

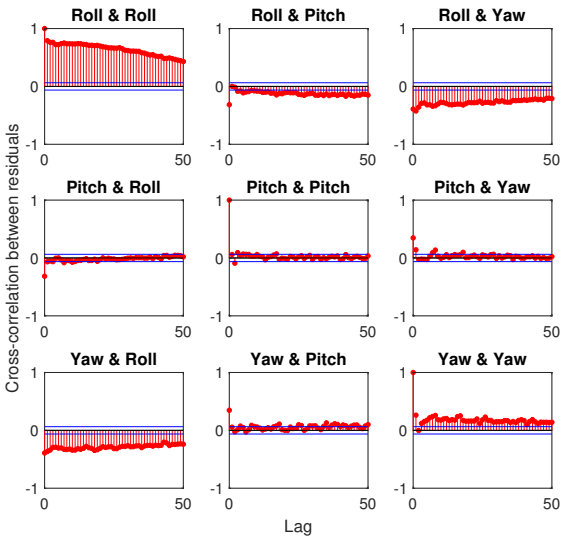

Fig. 16 Crosscorrelation of the roll, pitch and yaw residuals generated by healthy aircraft model for rotor 2 failure

Neural network 2 is trained with cross-correlation functions up to a maximum lag of 50 of residuals obtained from filtering signals of 5s length in the fault compensated phase through the healthy aircraft model (M_0). The cross-correlation of the roll, pitch and yaw residuals for different rotor failures have differentiating patterns (as shown in Figs. 15 - 17) which aids in fault classification. However, if the attitude signals of even longer length (such as 10 s) are used to train this network, its accuracy reduces to 83.78% as opposed to 99.97% accurate current network. The details of the 2 neural networks are given in Table 7.

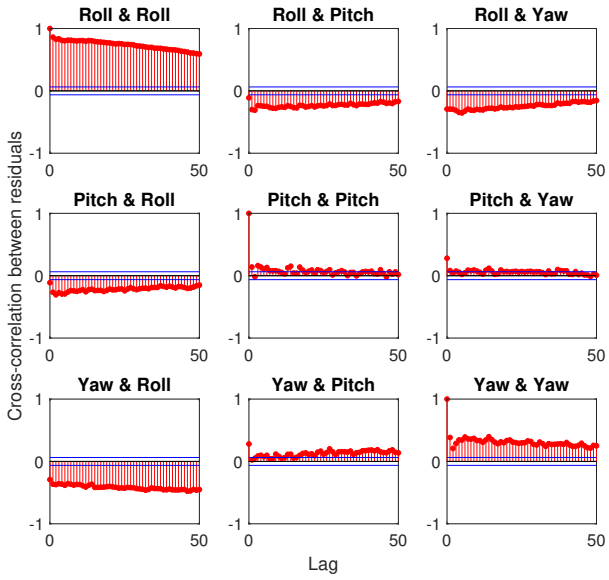

Fig. 17 Crosscorrelation of the roll, pitch and yaw residuals generated by healthy aircraft model for rotor 6 failure

Table 7 Details of the trained neural networks

Neural network 1		
Input Type	:	Transient Roll, Pitch and Yaw signals of length 0.2s ($N = 21$ samples) each
Input Layer Size	:	63
Training Function	:	Scaled Conjugate Gradient
Hidden Layer Size	:	5
Output Classes	:	4 (Healthy, Rotor 1,2 or 6 failures)
Cost Function	:	Cross-Entropy
Activation Function	:	1st layer - Hyperbolic Tangent Function , 2nd Layer - Softmax
Performance	:	7.0×10^{-7}
Neural network 2		
Input Type	:	Cross-correlation between residuals for maximum lag = 50
Input Layer Size	:	459
Training Function	:	Conjugate Gradient Backpropagation
Hidden Layer Size	:	5
Output Classes	:	3 (Rotor 1,2 or 6 failures)
Cost Function	:	Cross-Entropy
Activation Function	:	1st layer - Hyperbolic Tangent Function , 2nd Layer - Softmax
Performance	:	5.9×10^{-12}

2. Neural networks based Fault Detection and Identification

For online FDI, aircraft attitude signals of 0.2 s updated every 0.1 s have been input to Neural Network 1 until a fault is detected and identification follows with the transient signals. The fault detection and identification takes less than 0.4 s from the instant of rotor failure. The computation time required is less than 0.02 s, which is less than the window update time, making it suitable for online monitoring.

If a fault is encountered, the variance of the signals are monitored until steady state is reached as discussed in

Section VII.B.2. Once steady state is reached, signals of 5 s length (updated every 0.1 s), along with the vector time series model for the healthy aircraft (M_0), are utilized to identify faults with Neural Network 2. The computation time to evaluate the cross-correlation function from the residuals to classify the fault requires less than 0.08 s. Hence, this can be applied for online FDI.

The summary of results for fault detection and fault classification using neural networks is given in Tables 8 and 9.

Table 8 Fault detection results for neural networks

Healthy	Failure cases		
	Rotor 1	Rotor 2	Rotor 6
False Alarms	Missed Faults		
0/0/0	0/0/0	0/0/0	0/0/0

False Alarms for severe/moderate/light levels of turbulence out of 100 cases each
Missed Faults for severe/moderate/light levels of turbulence out of 100 cases each

Table 9 Confusion matrix for fault classification by neural networks

		Signals for failure of		
		Rotor 1	Rotor 2	Rotor 6
Outputs	Rotor 1	99.87/99.84/99.94	0.13/0.16/0.06	0/0/0
	Rotor 2	0.55/0.60/0.34	99.13/99.17/99.53	0.31/0.23/0.13
	Rotor 3	0.36/0.37/0.36	0.94/0.79/0.80	98.70/98.84/98.88

Fault Classification for severe/moderate/light levels of turbulence in percentage

D. Comparison between the different methods of Fault Detection and Identification

Knowledge based methods can detect and identify rotor failures fast and accurately, but are highly dependent on the signal recorded very close to initiation of rotor failure. If the sampling rate is not high enough, the initial deviation of signals due to abrupt rotor failure will be missed and this method will show poor performance. Also, for multicopters with a large number of rotors, it can become difficult to identify distinct patterns for each failure mode, along with the difficulty of multiple confidence intervals. This method is able to make single decision in case of rotor failure, for the entire flight time. The false alarm percentage or the number of times it detects failure even in case of healthy aircraft is 1.66%, which is much higher than the other FDI methods. The computation time for this method is the least among the other methods.

Statistical methods employing Vector Autoregressive models with residual based decision making are excellent for fast and accurate fault detection and distinguishing the healthy from fault-compensated states (even after the transient has receeded). For fault identification, time series models for each type of failure needs to be estimated. This method can be applied only to stationary signals (signals without any transient response) delaying the fault classification. Also, it has been observed that signal length 20 s gives failure classification accuracy of 99.6%. Whereas, the accuracy reduces significantly with the confusion between rotor 2 and 6 failures (classified as both failures simultaneously) up to 56% when shorter signal lengths (5 s) are used for online monitoring. The computation time for this method is highest among the other methods as there are 9 hypothesis tests to be performed for each decision. When run online, it can make multiple decisions throughout the flight time.

Neural networks can detect and identify faults from the transient signals just after the instant of rotor failure. Also, when the steady state is reached, the cross-correlation for residuals generated from filtering signals through healthy time series models can be used to classify faults with 99.3% accuracy. With less computation time (<0.08s) it is ideal for online FDI and does not require model identification for different rotor failures.

VIII. Conclusions

- Knowledge based methods detect and identify faults fast provided the sampling rate of signals are high enough. This method is effective only for lower number of fault classes and in case of abrupt and complete rotor failures.
- Statistical time series methods for rotor fault detection in multicopters achieve fast and accurate fault detection based on (i) ambient (white) excitation and aircraft attitude signals, (ii) statistical model building, and (iii) statistical decision making under uncertainty and different levels of turbulence.
- Fault identification by statistical time series method requires multiple models for different rotor failures. Decision making takes longer time as the hypothesis tests increase with number of fault classes. Also, the accuracy of this method depends on the length of current signals (number of samples). Using longer signals is observed to result in improved accuracy.
- Neural networks can detect and identify faults fast and accurately with transient signals. However, when trained with post-failure compensated signals, neural networks have lower accuracy in classifying rotor failures.
- Utilizing difference between cross-correlation functions of the signal residuals obtained from filtering through the healthy time-series model for different rotor failure cases, fault identification is possible. Neural networks trained on the cross-correlations functions results in 99.3% accurate fault identification with fault-compensated, steady state signals. This method is more accurate than fault identification with statistical time-series methods in online monitoring using shorter signal length. Moreover, it requires only one model for a healthy aircraft for fault identification.

Acknowledgments

This work is carried out at Rensselaer Polytechnic Institute under the Army/Navy/NASA Vertical Lift Research Center of Excellence (VLRCOE) Program, grant number W911W61120012, with Dr. Mahendra Bhagwat and Dr. William Lewis as Technical Monitors.

References

[1] Frangenberg, M., Stephan, J., and Fichter, W., "Fast Actuator Fault Detection and Reconfiguration for Multicopters," *AIAA Guidance, Navigation, and Control Conference*, AIAA, 2015. doi:10.2514/6.2015-1766.

[2] Heredia, G., and Ollera, A., "Sensor Fault Detection in Small Autonomous Helicopters using Observer/Kalman Filter Identification," *IEEE International Conference on Mechatronics, Malaga, Spain*, 2009.

[3] McKay, M., Niemiec, R., and Gandhi, F., "Post-Rotor-Failure-Performance of a Feedback Controller for a Hexacopter," *American Helicopter Society 74th Annual Forum, Phoenix, AZ*, AHS, 2018.

[4] Stepanyan, V., Krishnakumar, K., and Bencomo, A., "Identification and Reconfigurable Control of Impaired Multi-Rotor Drones," *AIAA Science and Technology Forum and Exposition*, 2016.

[5] Qi, X., Theillol, D., Qi, J., Zhang, Y., and Han, J., "A Literature Review on Fault Diagnosis Methods for Manned and Unmanned Helicopters," *International Conference on Unmanned Aircraft Systems*, 2013.

[6] Fassois, S., and Kopsaftopoulos, F., *New Trends in Structural Health Monitoring*, Springer, 2013, Chap. Statistical Time Series Methods for Vibration Based Structural Health Monitoring, pp. 209–264. doi:10.1007/978-3-7091-1390-5.

[7] Kopsaftopoulos, F. P., and Fassois, S. D., "Scalar and Vector Time Series Methods for Vibration Based Damage Diagnosis in a Scale Aircraft Skeleton Structure ," *Journal of Theoretical and Applied Mechanics*, Vol. 49, No. 4, 2011.

[8] Samara, P. A., Fouskitakis, G. N., Sakellariou, J. S., and Fassois, S. D., "A Statistical Method for the Detection of Sensor Abrupt Faults in Aircraft Control Systems," *IEEE Transactions on Control Systems Technology*, Vol. 16, No. 4, 2008, pp. 789–798. doi:10.1109/TCST.2007.903109.

[9] Kopsaftopoulos, F. P., and Fassois, S. D., "A vibration model residual-based sequential probability ratio test framework for structural health monitoring," *Structural Health Monitoring*, Vol. 14, No. 4, 2015, pp. 359–381.

[10] Dimogianopoulos, D. G., Hios, J. D., and Fassois, S. D., "FDI for Aircraft Systems Using Stochastic Pooled-NARMAX Representations: Design and Assessment," Vol. 17, No. 6, 2009, pp. 1385–1397.

[11] Kopsaftopoulos, F. P., and Fassois, S. D., "Helicopter Rotor System Fault Detection Using Physics-Based Model and Neural Networks," *AIAA Journa*, Vol. 36, No. 6, 1998, pp. 1078–1086.

[12] Morel, H., Ouladsine, M., Krysinski, T., and Brun-Picard, D., "Defect detection and tracing on helicopter rotors by artificial neural networks," *IEEE Advanced Process Control Applications for Industry Workshop, Vancouver, Canada*, 2005.

[13] Dutta, A., McKay, M., Kopsaftopoulos, F., and Gandhi, F., "Rotor Fault Detection and Identification on a Hexacopter Based on Statistical Time Series Methods," *Vertical Flight Society 75th Annual Forum, Philadelphia, PA*, AHS, 2019.

[14] Peters, D., and He, C., "A Finite-State Induced Flow Model for Rotors in Hover and Forward Flight," *American Helicopter Society 43rd Annual Forum, St. Louis, MO*, AHS, 1987.

[15] Hakim, T. M. I., and Arifianto, O., "Implementation of Dryden Continuous Turbulence Model into Simulink for LSA-02 Flight Test Simulation," *Journal of Physics: Conference Series 1005(2018) 012017*, 2018.

[16] Söderström, T., and Stoica, P., *System Identification*, Prentice–Hall, 1989.

[17] Lütkepohl, H., *New Introduction to Multiple Time Series Analysis*, Springer-Verlag Berlin, 2005.

[18] Fassois, S. D., "Parametric identification of vibrating structures," *Encyclopedia of Vibration*, edited by S. Braun, D. Ewins, and S. Rao, Academic Press, 2001, pp. 673–685.

[19] Ljung, L., *System Identification: Theory for the User*, 2nd ed., Prentice–Hall, 1999.